

Tripartite continuous-variable entanglement of NOPA system

Chao-Ying Zhao(赵超樱), Cheng-Mei Zhang(张成梅)

Citation: Chin. Phys. B . 2018, 27(8): 084204. **doi:** 10.1088/1674-1056/27/8/084204

Journal homepage: http://cpb.iphy.ac.cn; http://iopscience.iop.org/cpb

What follows is a list of articles you may be interested in

Three-mode optomechanical system for angular velocity detection

Kai Li(李凯), Sankar Davuluri, Yong Li(李勇)

Chin. Phys. B . 2018, 27(8): 084203. **doi:** 10.1088/1674-1056/27/8/084203

Quantum feedback cooling of two trapped ions

Shuo Zhang(张硕), Wei Wu(吴伟), Chun-Wang Wu(吴春旺), Feng-Guang Li(李风光), Tan Li(李坦), Xiang Wang(汪翔), Wan-Su Bao(鲍皖苏)

Chin. Phys. B . 2017, 26(7): 074205. **doi:** 10.1088/1674-1056/26/7/074205

Generation of a squeezed state at 1.55 μ with periodically poled $LiNbO_3$

Liu Qin, Feng Jin-Xia, Li Hong, Jiao Yue-Chun, Zhang Kuan-Shou

Chin. Phys. B . 2012, 21(10): 104204. **doi:** 10.1088/1674-1056/21/10/104204

Tripartite continuous-variable entanglement of NOPA system*

Chao-Ying Zhao(赵超樱)[1,2,†] and Cheng-Mei Zhang(张成梅)[3]

[1] College of Science, Hangzhou Dianzi University, Hangzhou 310018, China
[2] State Key Laboratory of Quantum Optics and Quantum Optics Devices, Institute of Opto-Electronics, Shanxi University, Taiyuan 030006, China
[3] Nokia Solutions and Networks, Hangzhou 310053, China

(Received 12 December 2017; revised manuscript received 7 March 2018; published online 10 July 2018)

We investigate the fundamental limits to the achievable tripartite continuous-variable (CV) entanglement criterion of a generalized V_1 criterion. Our numerical simulation results show that the non-degenerate eigenvalues do effect the performances of the estimated minimum variances. From below the threshold to above the threshold, with the increase of the pump parameter, the tripartite CV entanglement gradually disappears. The different off-diagonal elements seriously distort the weights for entanglement. We can obtain a good tripartite CV entanglement by appropriately controlling the values of off-diagonal elements ε_{ij}.

Keywords: continuous-variable entanglement, generalized V_1 criterion, non-degenerate eigenvalues

PACS: 42.50.Lc, 42.65.Lm **DOI:** 10.1088/1674-1056/27/8/084204

1. Introduction

Optical parametric process is one of the most effective techniques to realize entangled states. All bipartite entangled states are useful for quantum teleportation,[1] dense coding,[2] cryptography,[3] tomography,[4] entanglement swapping,[5] quantum key distribution,[6] quantum computation, and quantum information process.[7,8] Aoki *et al.* first theoretically proposed that a tripartite continuous-variable (CV) entangled state should be generated by combining three independent squeezed vacuum states.[9] Jing *et al.* proposed a tripartite entangled state of a bright optical field should be experimentally produced by using an Einstein–Podolsky–Rosen entangled state and linear optics.[10] Pfister *et al.* showed theoretically a tripartite CV entangled state in a second-order nonlinear medium with concurrent interactions.[11] Guo *et al.* theoretically produced tripartite entanglement by using a parametric down conversion and sum-frequency process.[12] Furthermore, Pennarun *et al.* predicted tripartite CV entanglement by using cascaded down-conversion and sum-frequency process.[13] Allevi *et al.* experimentally demonstrated the nonclassical photon number correlations in tripartite CV states[14] and then investigated the process of entanglement transfer.[15] Weinstein explored the tripartite entanglement witnesses and entanglement sudden death.[16] Wang *et al.* experimentally investigated tripartite entanglement in a cascaded four-wave-mixing (FWM) system.[17] Wang *et al.* experimentally demonstrated three quantum correlated beams and quantum steering by using a phase-sensitive cascaded FWM process.[18,19] Zheng *et al.* investigated different kinds of entanglement in an FWM process with a degenerate pump.[20] Qin *et al.* experimentally produced multiple quantum correlated beams in a hot rubidium vapor.[21] Furthermore, Daems *et al.* presented spatial tripartite entanglement.[22]

Several schemes in which the temporal multipartite entanglement was realized[23] were proposed as result of parametric interaction, such as cascaded, concurrent,[24] interlinked,[25] or consecutive parametric interactions,[26] coupled parametric down-conversions.[27] Lv and Jing investigated quadripartite entanglement by using a cascaded FWM process.[28] We investigated theoretically CV multipartite entanglement in a non-degenerate optical parametric amplification (NOPA) system.[29–31] We obtained the generalized criterion V_1 for multipartite entanglement. Here we set all off-diagonal elements to be equal, i.e., $\varepsilon_{12}=\varepsilon_{21}^{*}=\varepsilon_{13}=\varepsilon_{31}^{*}=\varepsilon_{23}=\varepsilon_{32}^{*}=\varepsilon_0$. In this paper, we will take off-diagonal elements to be different, i.e., $(\varepsilon_{12}=\varepsilon_{21}^{*})\neq(\varepsilon_{13}=\varepsilon_{31}^{*})\neq(\varepsilon_{23}=\varepsilon_{32}^{*})$, which act as the conditions under which the realistic tripartite entanglement for this system takes place. We can obtain a good tripartite CV entanglement by appropriately controlling the values of off-diagonal elements ε_{ij}.

2. Criteria for tripartite entanglement

In the p representation, the Hamiltonian of the system in the rotating frame at the driving frequency is given by the following expression[29–31]

$$H=H_0+V+W,$$

*Projected supported by the National Natural Science Foundation of China (Grant No. 11504074) and the Science Fund from the State Key Laboratory of Quantum Optics and Quantum Optics Devices, Shanxi University, Shanxi, China (Grant No. KF201601).

†Corresponding author. E-mail: zchy49@hdu.edu.cn

© 2018 Chinese Physical Society and IOP Publishing Ltd

where

$$\begin{aligned} H_0 &= \hbar\omega_0 a_0^\dagger a_0 + \sum_{m=1}^{N} \hbar\omega_m a_m^\dagger a_m + \mathrm{i}\hbar(E\,\mathrm{e}^{-\mathrm{i}\omega_L t} a_0^\dagger - E^*\,\mathrm{e}^{\mathrm{i}\omega_L t} a_0) \\ &\quad + \sum_j \sum_{m=1}^{N} \hbar\omega_j B_{jm}^\dagger B_{jm}, \\ V &= \hbar \sum_j \sum_{m=1}^{N} k_j B_{jm} a_m^\dagger + \hbar \sum_j \sum_{m=1}^{N} k_j^* B_{jm}^\dagger a_m, \\ W &= \frac{\mathrm{i}\hbar}{2} \sum_{j\neq k}^{N} (2\varepsilon_{jk} a_j^\dagger a_k^\dagger - 2\varepsilon_{kj} a_j a_k), \end{aligned} \tag{1}$$

where the creation (annihilation) operators $a_0^\dagger$ (a_0), $a_j^\dagger$ (a_j), and $a_k^\dagger$ (a_k) at frequencies ω_0, ω_j, and ω_k refer to the pump, signal, and idler field, respectively; H_0 describes the Hamiltonian of the heat bath; V represents the interaction Hamiltonian of the signal, idler field, and heat bath; W represents the interaction Hamiltonian between pump field α_0 (included in gain factor $\varepsilon_{jk} = \chi_{jk}\alpha_0$) and signal photons $a_j^\dagger$, and idler photons $a_k^\dagger$.

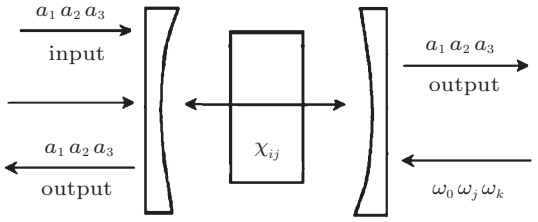


Fig. 1. Input–output relation in NOPA system, the modes a_1, a_2, a_3, and frequencies ω_0, ω_j, ω_k refer to pump, signal, and idler field, respectively. χ_{ij} represents the effective second-order susceptibility of nonlinear crystal in NOPA system.

Assuming perfect phase-matching, ignoring pump depletion, and setting output loss rates to be equal, i.e., $k_j = k$, we will first examine a simplified analytical model for the propagation of fields. Dynamical equations for a non-degenerate optical parametric process in compound modes are

$$\frac{\mathrm{d}}{\mathrm{d}t} a_j = -k a_j + \sum_{j\neq k} \varepsilon_{jk} a_k^\dagger, \quad \frac{\mathrm{d}}{\mathrm{d}t} a_k^\dagger = -k a_k^\dagger + \sum_{j\neq k} \varepsilon_{jk} a_j. \tag{2}$$

In the positive-p representation, the semi-classical equations of motion for three degenerate parametric modes a_1, a_2, a_3[30] can be obtained by solving the Fokker–Planck equation. Here $\varepsilon_{12} = \varepsilon_{21}^* \neq \varepsilon_0$, $\varepsilon_{13} = \varepsilon_{31}^* \neq \varepsilon_0$, $\varepsilon_{23} = \varepsilon_{32}^* \neq \varepsilon_0$,

$$\begin{aligned} \mathrm{Det} &= \begin{vmatrix} -\lambda_1 & -\varepsilon_{12} & -\varepsilon_{13} \\ -\varepsilon_{21}^* & -\lambda_1 & -\varepsilon_{23} \\ -\varepsilon_{31}^* & -\varepsilon_{32}^* & -\lambda_1 \end{vmatrix} \\ &= -\lambda^3 + (\varepsilon_{12}^2 + \varepsilon_{23}^2 + \varepsilon_{13}^2)\lambda - 2\varepsilon_{12}\varepsilon_{23}\varepsilon_{13} \\ &= 0, \end{aligned}$$

where

$$\theta = \frac{1}{3} \arccos\left[\varepsilon_{12}\varepsilon_{23}\varepsilon_{13} \left(-\frac{\varepsilon_{12}^2 + \varepsilon_{23}^2 + \varepsilon_{13}^2}{3} \right)^{-3/2} \right],$$

$$\begin{aligned} \lambda_1 &= \sqrt{-\frac{4(\varepsilon_{12}^2 + \varepsilon_{23}^2 + \varepsilon_{13}^2)}{3}} \cos[\theta], \\ \lambda_2 &= \sqrt{-\frac{4(\varepsilon_{12}^2 + \varepsilon_{23}^2 + \varepsilon_{13}^2)}{3}} \cos\left[\theta + \frac{2\pi}{3}\right] \\ &= -\sqrt{-\frac{4(\varepsilon_{12}^2 + \varepsilon_{23}^2 + \varepsilon_{13}^2)}{3}} \left(\frac{\lambda_1}{2} + \frac{\sqrt{3}}{2}\sqrt{1-\lambda_1^2} \right), \\ \lambda_3 &= \sqrt{-\frac{4(\varepsilon_{12}^2 + \varepsilon_{23}^2 + \varepsilon_{13}^2)}{3}} \cos\left[\theta + \frac{4\pi}{3}\right] \\ &= -\sqrt{-\frac{4(\varepsilon_{12}^2 + \varepsilon_{23}^2 + \varepsilon_{13}^2)}{3}} \left(\frac{\lambda_1}{2} - \frac{\sqrt{3}}{2}\sqrt{1-\lambda_1^2} \right). \end{aligned} \tag{3}$$

Due to the fact that the eigenvalues are different from each other, we can use the eigensolution to construct a transfer matrix u_{ij},[29] which connects the output (b_1, b_2, b_3) and input (a_1, a_2, a_3) and satisfies

$$\begin{aligned} u_{ij} \begin{pmatrix} 0 & -\varepsilon_{12} & -\varepsilon_{13} \\ -\varepsilon_{21}^* & 0 & -\varepsilon_{23} \\ -\varepsilon_{31}^* & -\varepsilon_{32}^* & 0 \end{pmatrix} u_{ij}^{-1} &= \begin{pmatrix} \lambda_1 & 0 & 0 \\ 0 & \lambda_2 & 0 \\ 0 & 0 & \lambda_3 \end{pmatrix}, \\ u_{ij}(-\lambda_i) &= \frac{\Delta_{ij}(-\lambda_i)}{\sqrt{\sum_{j=1}^{3} \Delta_{ij}^2(-\lambda_i)}}. \end{aligned} \tag{4}$$

Here $\Delta_{ij}(-\lambda_i)$ is the cofactor of the determinant.

NOPA with modes a_1, a_2, a_3 can be resolved into a combination of DOPA1 (k, λ_1) with mode b_1, DOPA2 (k, λ_2) with mode b_2 and DOPA1 (k, λ_3) with mode b_3[29]

$$\begin{aligned} &\begin{pmatrix} L & \lambda_1 \\ \lambda_1 & L \end{pmatrix} \begin{pmatrix} b_1 \\ b_1^\dagger \end{pmatrix} = 0, \quad \begin{pmatrix} L & \lambda_2 \\ \lambda_2 & L \end{pmatrix} \begin{pmatrix} b_2 \\ b_2^\dagger \end{pmatrix} = 0, \\ &\begin{pmatrix} L & \lambda_3 \\ \lambda_3 & L \end{pmatrix} \begin{pmatrix} b_3 \\ b_3^\dagger \end{pmatrix} = 0, \end{aligned} \tag{5}$$

where $L = \mathrm{d}/\mathrm{d}t + k$, in the case of $k = 0$, $b_i = \beta_i + \mathrm{i}\tilde{\beta}_i$, we write out the quantum fluctuations of b_1 and b_2

$$\begin{aligned} &X_1(l) = \beta_1 + \tilde{\beta}_1, \;\; Y_1(l) = \beta_1 - \tilde{\beta}_1, \;\; X_2(l) = \beta_2 + \tilde{\beta}_2, \\ &Y_2(l) = \beta_2 - \tilde{\beta}_2, \;\; X_3(l) = \beta_3 + \tilde{\beta}_3, \;\; Y_3(l) = \beta_3 - \tilde{\beta}_3. \end{aligned} \tag{6}$$

Here $X_1(0)$, $Y_2(0)$, and $Y_3(0)$ are the input amplitudes, and we have $\langle [X_1(0)]^2 \rangle = \langle [Y_2(0)]^2 \rangle = \langle [Y_3(0)]^2 \rangle = 1$, $\langle X_1(0) \rangle = \langle Y_2(0) \rangle = \langle Y_3(0) \rangle = 0$, $\langle X_1(0) Y_2(0) \rangle = \langle X_1(0) Y_3(0) \rangle = 0$. For the non-degenerate optical fields, the measurements of the idler amplitudes $Y_2(l)$ and $Y_3(l)$ will infer the result for the signal amplitude $X_1(l)$.

During the interaction time $t = l/c$, quantum fluctuation becomes

$$\begin{aligned} \langle X_1^2 \rangle &= \cosh^2[\lambda_1 t] + \frac{1}{2}(\sinh^2[\lambda_2 t] + \sinh^2[\lambda_3 t]), \\ \langle Y_2^2 \rangle &= \sinh^2[\lambda_1 t] + \cosh^2[\lambda_2 t], \\ \langle Y_3^2 \rangle &= \sinh^2[\lambda_1 t] + \cosh^2[\lambda_3 t], \end{aligned} \tag{7}$$

The output signal amplitude X_1 and idler amplitudes Y_2 and Y_3 satisfy

$$\langle X_1 Y_2\rangle = \frac{1}{\sqrt{2}}(\cosh[\lambda_1 t]\sinh[\lambda_1 t]+\cosh[\lambda_2 t]\sinh[\lambda_2 t]),$$
$$\langle X_1 Y_3\rangle = \frac{1}{\sqrt{2}}(\cosh[\lambda_1 t]\sinh[\lambda_1 t]+\cosh[\lambda_3 t]\sinh[\lambda_3 t]). \quad (8)$$

Equations (7) and (8) correspond to the case of $k \to 0$. Considering the case of loss $k > 0$ and adding the vacuum fluctuations, the quantum fluctuations are

$$\begin{aligned}\langle X_1^2\rangle &= 1+\frac{1}{2}[\frac{\lambda_1}{2(k-\lambda_1)}(1-\exp[-2(k-\lambda_1)t])\\ &-\frac{\lambda_1}{2(k+\lambda_1)}(1-\exp[-2(k+\lambda_1)t])]\\ &+\frac{1}{4}[\frac{\lambda_2}{2(k-\lambda_2)}(1-\exp[-2(k-\lambda_2)t])\\ &-\frac{\lambda_2}{2(k+\lambda_2)}(1-\exp[-2(k+\lambda_2)t])]\\ &+\frac{1}{4}[\frac{\lambda_3}{2(k-\lambda_3)}(1-\exp[-2(k-\lambda_3)t])\\ &-\frac{\lambda_3}{2(k+\lambda_3)}(1-\exp[-2(k+\lambda_3)t])],\\ \langle Y_2^2\rangle &= 1+\frac{1}{2}[\frac{\lambda_2}{2(k-\lambda_2)}(1-\exp[-2(k-\lambda_2)t])\\ &-\frac{\lambda_2}{2(k+\lambda_2)}(1-\exp[-2(k+\lambda_2)t])]\\ &+\frac{1}{2}[\frac{\lambda_1}{2(k-\lambda_1)}(1-\exp[-2(k-\lambda_1)t])\\ &-\frac{\lambda_1}{2(k+\lambda_1)}(1-\exp[-2(k+\lambda_1)t])],\\ \langle Y_3^2\rangle &= 1+\frac{1}{2}[\frac{\lambda_3}{2(k-\lambda_3)}(1-\exp[-2(k-\lambda_3)t])\\ &-\frac{\lambda_3}{2(k+\lambda_3)}(1-\exp[-2(k+\lambda_3)t])]\\ &+\frac{1}{2}[\frac{\lambda_1}{2(k-\lambda_1)}(1-\exp[-2(k-\lambda_1)t])\\ &-\frac{\lambda_1}{2(k+\lambda_1)}(1-\exp[-2(k+\lambda_1)t])]. \quad (9)\end{aligned}$$

The correlations between X_1 and Y_2, and between X_1 and Y_3 satisfy

$$\begin{aligned}\langle X_1 Y_2\rangle &= \frac{1}{2\sqrt{2}}[\frac{\lambda_1}{2(k+\lambda_1)}(1-\exp[-2(k+\lambda_1)t])\\ &+\frac{\lambda_1}{2(k-\lambda_1)}(1-\exp[-2(k-\lambda_1)t]]\\ &+\frac{1}{2\sqrt{2}}[\frac{\lambda_2}{2(k+\lambda_2)}(1-\exp[-2(k+\lambda_2)t])\\ &+\frac{\lambda_2}{2(k-\lambda_2)}(1-\exp[-2(k-\lambda_2)t])],\\ \langle X_1 Y_3\rangle &= \frac{1}{2\sqrt{2}}[\frac{\lambda_1}{2(k+\lambda_1)}(1-\exp[-2(k+\lambda_1)t])\\ &+\frac{\lambda_1}{2(k-\lambda_1)}(1-\exp[-2(k-\lambda_1)t])]\\ &+\frac{1}{2\sqrt{2}}[\frac{\lambda_3}{2(k+\lambda_3)}(1-\exp[-2(k+\lambda_3)t])\\ &+\frac{\lambda_3}{2(k-\lambda_3)}(1-\exp[-2(k-\lambda_3)t])]. \quad (10)\end{aligned}$$

We can use the solutions of X_1, Y_2, and Y_3 to find the quadrature variances[29]

$$\begin{aligned}V_1 &= [V_1(g_2\cdots g_n)]_{\min}\\ &= \langle X_1^2\rangle - \left(\frac{\langle X_1 Y_2\rangle^2}{\langle Y_2^2\rangle}+\frac{\langle X_1 Y_3\rangle^2}{\langle Y_3^2\rangle}\right). \quad (11)\end{aligned}$$

The key point is that the entanglement exists among the signal amplitude X_1 (located at position 1), the idler phase Y_2 (located at position 2), and Y_3 (located at position 3). The amplitude and phase components X_1, Y_2, and Y_3 are generated through the NOPA system interaction involved in W of Eq. (1). Now we use Eq. (11) to monitor the evolutions of signal and idler modes of the NOPA system and regard the violation of $V_1 \geq 1$ as the sufficient condition of entanglement.

3. Numerical calculation

The variations of minimum variance V_1 with interaction time t for $\varepsilon_{12} = 1.5\varepsilon_0$, $\varepsilon_{13} = 0.6\varepsilon_0$, $\varepsilon_{23} = \varepsilon_0$ are investigated and shown in Fig. 2.

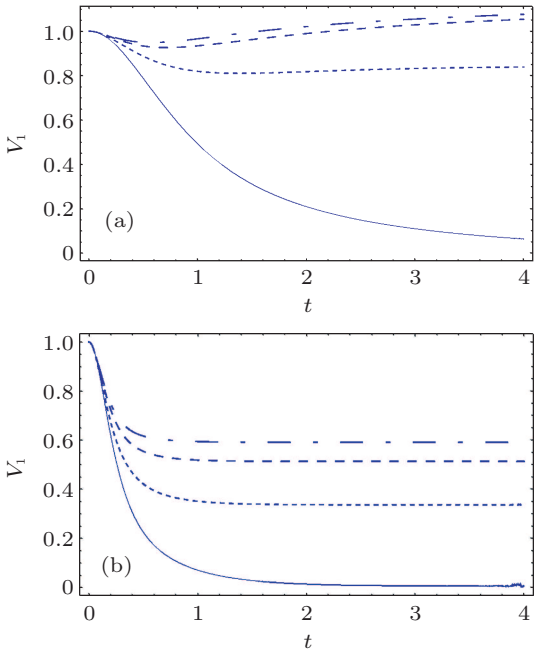


Fig. 2. (color online) Plots of variance V_1 versus t with (a) $\varepsilon_0 = 0.5$ and (b) 2 for $k = 0$ (solid curve), 0.5 (narrow dashed curve), 0.9 (wide dashed curve), and 1.1 (dotted-dashed curve).

From below the threshold to above the threshold, the curves gradually merge, the position of the minimum variance turns gradually toward the left, and the value of minimum variance V_1 decreases. With the increase of loss k, two curves satisfy the condition $V_{1\min}$; $0.82 < 1$, and the entanglement disappears gradually. While four curves satisfy the condition $V_{1\min}$; $0.6 < 1$, the entanglement always appears.

Given pump parameter $\varepsilon_0 = 2$, the value of minimum variance V_1 changes with off-diagonal elements ε_{ij}. In Figs. 3(a)–3(c), four curves satisfy the condition $V_{1\min}$; $0.58, 0.7, 0.76 < 1$, respectively, so the entanglement always appears.

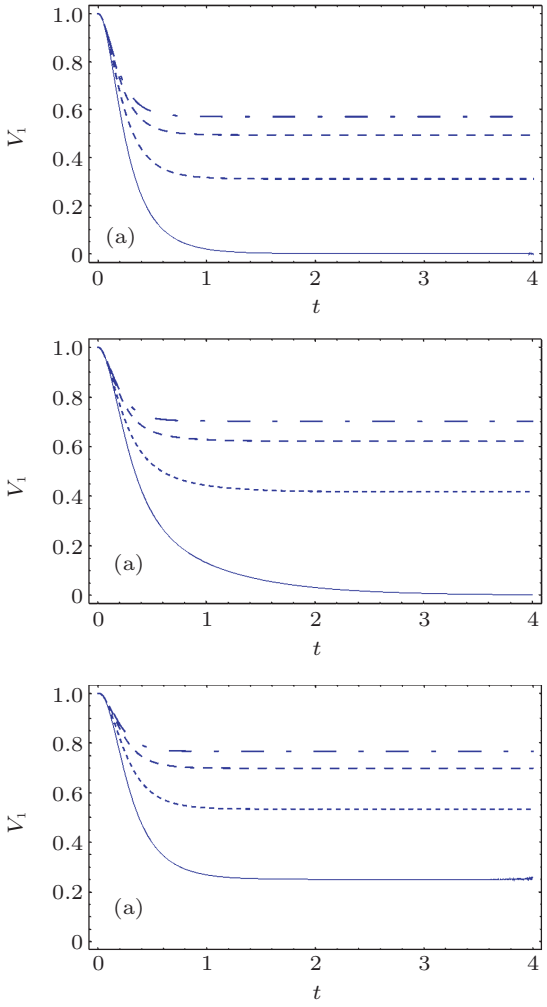


Fig. 3. (color online) Plots of variance V_1 versus t with $\varepsilon_0 = 2$ for $k = 0$ (solid curve), 0.5 (narrow dashed curve), 0.9 (wide dashed curve), and 1.1 (dashed–dotted curve), for the cases of panel (a): $\varepsilon_{12} = 1.5\varepsilon_0$, $\varepsilon_{13} = 0.6\varepsilon_0$, $\varepsilon_{23} = \varepsilon_0$; (b) $\varepsilon_{12} = 1.2\varepsilon_0$, $\varepsilon_{13} = 0.4\varepsilon_0$, $\varepsilon_{23} = 0.8\varepsilon_0$; (c) $\varepsilon_{12} = \varepsilon_0$, $\varepsilon_{13} = \varepsilon_0$, $\varepsilon_{23} = \varepsilon_0$.

4. Conclusions

In this paper, we use the minimum variance criterion to monitor the evolutions of signal and idler modes of a NOPA system with different off-diagonal elements, as these are the conditions under which there exists the realistic tripartite entanglement for this system. Our result is suitable for the whole region from below the threshold to above the threshold. For above the threshold, we can obtain a good tripartite CV entanglement by appropriately controlling the values of off-diagonal elements ε_{ij}.

References

[1] Furusawa A, Sorensen J L, Braunstein S L, Fuchs C A, Kimble H J and Polzik E S 1998 *Science* **282** 706
[2] Li X Y, Pan Q, Jing J T, Zhang J, Xie C D and Peng K C 2002 *Phys. Rev. Lett.* **88** 047904
[3] Silberhorn C, Korolkova N and Leuchs G 2002 *Phys. Rev. Lett.* **89** 167902
[4] D'Ariano G M and Presti P L 2001 *Phys. Rev. Lett.* **86** 4195
[5] Jia X J, Su X L, Pan Q, Gao J R, Xie C D and Peng K C 2004 *Phys. Rev. Lett.* **93** 250503
[6] Su X L, Wang W Z, Wang Y, Jia X J, Xie C D and Peng K C 2009 *Europhys. Lett.* **87** 20005
[7] Tan A H, Wang Y, Jin X L, Su X L, Jia X J, Zhang J, Xie C D and Peng K C 2008 *Phys. Rev. A* **78** 013828
[8] Yoshikawa J, Miwa Y, Huck A, Andersen U L, Loock P V and Furusawa A 2008 *Phys. Rev. Lett.* **101** 250501
[9] Aoki T, Takei N, Yonezawa H, Wakui K, Hiraoka T, Furusawa A and van Loock P 2003 *Phys. Rev. Lett.* **91** 080404
[10] Jing J, Zhang J, Yan Y, Zhao F, Xie C and Peng K 2003 *Phys. Rev. Lett.* **90** 167903
[11] Pfister O, Feng S, Jennings G, Pooser R and Xie D R 2004 *Phys. Rev. A* **70** 020302(R)
[12] Guo J, Zhai Z H and Gao J R 2010 *J. Opt. Soc. Am. B* **27** 518
[13] Pennarun C, Bradley A S and Olsen M K 2007 *Phys. Rev. A* **76** 063812
[14] Allevi A, Bondani M, Paris M G A and Andreoni A 2008 *Phys. Rev. A* **78** 063801
[15] Casagrande F, Lulli A and Paris M G A 2009 *Phys. Rev. A* **79** 022307
[16] Weinstein Y S 2009 *Phys. Rev. A* **79** 012318
[17] Wang H L, Zheng Z, Wang Y X and Jing J T 2016 *Opt. Express* **24** 23459
[18] Wang L, Wang H L, Li S J, Wang Y X and Jing J T 2017 *Phys. Rev. A* **95** 013811
[19] Wang L, Lv S C and Jing J T 2017 *Opt. Express* **25** 17457
[20] Zheng Z, Wang H L, Cheng B and Jing J T 2017 *Opt. Lett.* **42** 2754
[21] Qin Z Z, Cao L M, Wang H L, Marino A M, Zhang W P and Jing J T 2014 *Phys. Rev. Lett.* **113** 023602
[22] Daems D, Bernard F, Cerf N J and Kolobov M I 2010 *J. Opt. Soc. Am. B* **27** 447
[23] Lian Y M, Xie C D and Peng K C 2007 *New. J. Phys.* **9** 314
[24] Yu Y B, Xie Z D, Yu X Q, Li H X, Xu P, Yao H M and Zhu S N 2006 *Phys. Rev. A* **74** 042332
[25] Ferraro A, Paris M G A, Bondani M, Allevi A, Puddu E and Andreoni A 2004 *J. Opt. Soc. Am. B* **21** 1241
[26] Olsen M K and Bradley A S 2006 *Phys. Rev. A* **74** 063809
[27] Rodionov A V and Chirkin A S 2004 *JETP Lett.* **79** 253
[28] Lv S C and Jing J T 2017 *Phys. Rev. A* **96** 043873
[29] Zhao C Y, Tan W H, Xu J R and Ge F 2011 *J. Opt. Soc. Am. B* **28** 1067
[30] Zhao C Y 2017 *J. Mod. Opt.* **64** 52
[31] Zhao C Y 2017 *J. Mod. Opt.* **64** 150